Determination of Gamma Photon Absorption Characteristics of Rice Husk Ash–Doped Concrete as an Alternative Radiation Shielding Material

Aribisala Abdul-Jamiu [*1], *Umaru Ibrahim* [1], *Abdullahi A. Mundi* [1], *Idris M. Mustapha* [1] *and Atef El-Taher* [2]

[1]Department of Physics, Nasarawa State University, Keffi, P.M.B. 1022, Keffi, Nasarawa State, Nigeria.
[2] Department of Physics, Faculty of Science, Al-Azhar, University Assiut, Egypt.

Abstract: This study investigates the gamma photon absorption characteristics of rice husk ash (RHA)–doped concrete as a sustainable alternative to conventional cement concrete used for radiation shielding applications. Concrete composites containing 0–45 wt.% rice husk ash were fabricated and analyzed. Elemental compositions were determined using energy-dispersive X-ray fluorescence (EDXRF). Radiation shielding parameters were evaluated over a photon energy range of 0.1–15 MeV using the Phy-X/PSD software based on the Lambert–Beer law. The mass attenuation coefficient, half-value layer, tenth-value layer, and mean free path were determined. Results show that mass attenuation decreases with increasing photon energy, while HVL, TVL, and MFP increase. Increasing RHA content enhances attenuation performance. The effective atomic number decreases in the low-energy region and increases at higher energies. The results indicate that RHA-doped concrete is a promising, eco-friendly radiation shielding material.

Keywords: Rice husk ash, shielding, mass attenuation coefficient, and gamma radiation.

1 Introduction

Ionizing radiation constitutes a type of high-energy radiation characterized by its capacity to dislodge tightly bound electrons from atoms, thus generating ions [1-3]. This ionization process can have detrimental consequences for living cells and genetic material, posing potential risks to human health. Numerous sources of ionizing radiation, such as nuclear reactions, X-rays, and radioactive materials, can be encountered [4-6].

Chronic exposure to ionizing radiation, as seen in medical professionals, has been linked to an elevated risk of cancer, especially leukemia, thyroid cancer, breast cancer, and lung cancer [8-10]. Additionally, sensitive organs like the thyroid can be adversely affected by radiation exposure. Radiation therapy, a medical application of ionizing radiation, is utilized for cancer treatment, involving the focused application of high doses to tumor cells. Nevertheless, it is imperative to acknowledge that this therapy can also impact surrounding healthy tissues [11-15].

Radiation shielding materials are essential for reducing exposure to ionizing radiation in medical, industrial, and nuclear applications. Conventional shielding materials such as lead and ordinary concrete are widely used due to their high attenuation efficiency; however, lead presents toxicity concerns, while conventional concrete contributes significantly to environmental degradation due to cement production [16-17].

Recent research has increasingly focused on sustainable alternatives through the incorporation of agricultural and industrial waste materials into cementitious composites [18-19]. Rice husk ash (RHA), an abundant agricultural by-product rich in amorphous silica, has been shown to exhibit strong pozzolanic properties when used as a partial cement replacement [19]. The inclusion of RHA in concrete improves waste management and may enhance radiation attenuation properties due to its elemental composition.

Although RHA has been extensively studied for mechanical and durability performance in concrete, limited information exists regarding its gamma radiation shielding capability over a broad photon energy range. Therefore, this study aims to evaluate the gamma photon absorption

*Corresponding author e-mail: abdul_jamiu07@yahoo.com

characteristics of RHA-doped concrete using theoretical shielding calculations based on experimentally determined elemental compositions. Thermal stability and phase development are also examined to assess material suitability for shielding applications.

2 Experimental Procedure

2.1 Collection and Processing of Rice Husk Ash

Rice husk ash was collected from multiple rice milling locations in Keffi town, where rice husk waste is commonly generated. The ash was air-dried and sieved through a 2 mm mesh to remove coarse particles and ensure material uniformity, consistent with established processing methods for pozzolanic materials [8].

2.2 Preparation of RHA-Doped Concrete Samples

Concrete samples were prepared by partially replacing cement with rice husk ash at 0, 5, 10, 15, 20, 25, 30, 35, 40, and 45 wt.%. Granite and sand contents were kept constant across all mixtures. Mixing was performed using a laboratory mechanical mixer, and approximately 25 mL of water was added to each mixture to achieve homogeneity.

The fresh mixtures were cast into cylindrical molds of 2 cm diameter and 6 cm height, air-dried to constant mass, and subsequently oven-dried at 100 °C for 2 h to eliminate residual moisture.

2.3 Bulk Density Determination

The bulk density ρ of each composite was calculated as the ratio of sample mass to volume:

$$\rho = \frac{m}{V} \qquad 1$$

Density values were used as input parameters for radiation shielding calculations, as density significantly influences photon attenuation behavior [11].

2.4 Elemental Composition Analysis

Elemental compositions of the fabricated samples were determined using a Thermo Scientific ARL-QUANT'X energy-dispersive X-ray fluorescence (EDXRF) analyzer. Approximately 2 g of each sample was analyzed following standard XRF procedures, using certified reference materials for calibration. Elemental composition is a critical input for accurate shielding parameter calculations [9].

2.7 Radiation Shielding Assessment

Gamma radiation shielding parameters were calculated using the Phy-X/PSD online software, which applies the Lambert–Beer law:

$$I = I_0 e^{-\mu x} \qquad 2$$

where I is the transmitted photon intensity, I_o is the incident intensity, μ is the linear attenuation coefficient (cm^{-1}), and x is the material thickness (cm) [10].

The mass attenuation coefficient was calculated as:

$$\mu_m = \frac{\mu}{\rho} \qquad 3$$

The half-value layer (HVL), tenth-value layer (TVL), and mean free path (MFP) were computed using:

$$HVL = \frac{ln2}{\mu} \qquad 4$$

$$TVL = \frac{ln10}{\mu} \qquad 5$$

$$MFP = \frac{1}{\mu} \qquad 6$$

The effective atomic number Z_{eff} was determined by the software based on the weighted elemental composition of each sample [3].

3 Results and Discussion

The results of shielding parameters of the rice husk ash-doped concrete sample R0 - R9. The mass attenuation coefficient, linear attenuation coefficient, mean free path, half value thickness, and effective atomic number are analyzed.
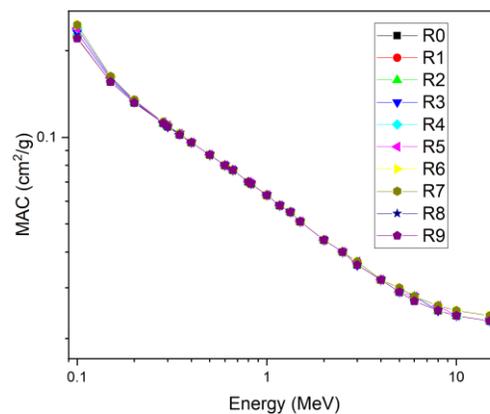

Fig.1: Comparison of the mass attenuation coefficient of the rice husk ash-doped concrete sample at various energies.

Figure 1 presents the comparison of the mass attenuation coefficient of the rice husk ash-doped concrete sample at various energies. The mass attenuation coefficient of the rice husk ash–doped concrete decreases steadily with increasing photon energy for all samples. Higher MAC values at low energies (0.1–0.5 MeV) are due to dominant photoelectric absorption, with slight improvements observed in samples containing higher RHA content. At intermediate and high energies, the MAC values converge for all samples as Compton scattering becomes dominant, making the effect of RHA content negligible. Overall, RHA incorporation enhances gamma attenuation mainly at low photon energies. Higher MAC values at low photon energies are attributed to the dominance of the photoelectric effect, which strongly depends on atomic number and photon energy [3]. At higher energies, Compton scattering dominates, leading to reduced variation among samples [20-26].
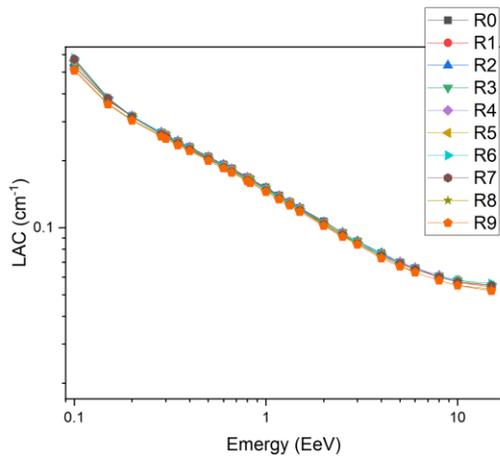

Fig.2: Comparison of the linear attenuation coefficient of the rice husk ash-doped concrete sample at various energies.

Figure 2 presents the comparison of the linear attenuation coefficient of the rice husk ash-doped concrete sample at various energies. The linear attenuation coefficient (LAC) of the rice husk ash–doped concrete decreases consistently with increasing photon energy for all samples, as shown in Table 4.3. At low photon energies (0.1–0.3 MeV), higher LAC values are observed due to the dominance of the photoelectric effect, which strongly depends on material density and elemental composition. In this region, samples with higher rice husk ash content (notably R4–R7) exhibit relatively higher LAC values, indicating improved shielding performance compared to the control sample (R0). As photon energy increases beyond this range, the LAC values gradually decrease, and the differences among samples become less pronounced. This convergence at intermediate and high energies reflects the dominance of Compton scattering, where attenuation is mainly governed by electron density rather than compositional variations.

Overall, the results demonstrate that incorporating rice husk ash enhances gamma-ray attenuation, particularly at low energies, while at higher energies the attenuation behavior is largely independent of RHA content [9].
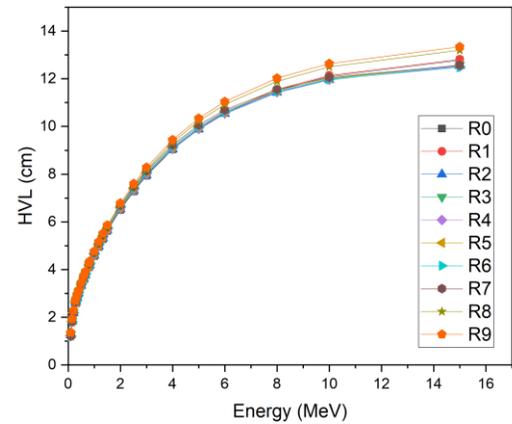

Fig.3: Comparison of half value layer of the rice husk ash-doped concrete at various energies.

Figure 3 presents the comparison of half value layer of the rice husk ash-doped concrete at various energies. The half-value layer of rice husk ash–doped concrete increases with photon energy, indicating reduced photon interaction at higher energies. At low energies (0.1–0.3 MeV), higher RHA content lowers HVL, showing improved shielding due to enhanced photoelectric absorption from increased effective atomic number and density. At higher energies, HVL rises for all samples, and differences among them diminish, as Compton scattering dominates. Overall, RHA

improves gamma-ray attenuation primarily at low to medium energies, while sufficient material thickness is essential at higher energies.
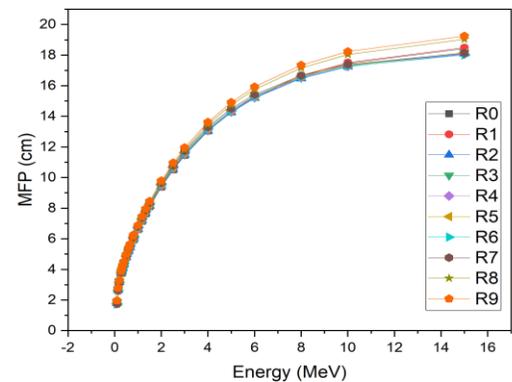

Fig.4: Comparison of the mean free path of rice husk ash-doped concrete at various energies.

Figure 4 presents the comparison of the mean free path of rice husk ash-doped concrete at various energies. The mean free path (MFP) of the rice husk ash–doped concrete increases with photon energy for all samples, as shown in Table 4.6. At low photon energies (0.1–0.3 MeV), samples with higher RHA content (R4–R7) exhibit shorter MFP values compared to the control (R0), indicating more frequent photon interactions and enhanced shielding efficiency. As photon energy increases, MFP values rise steadily for all samples, reflecting the reduced probability of photon interactions at higher energies. Differences between samples become more noticeable at higher energies, with samples containing lower RHA content showing slightly shorter MFP, suggesting that material composition has a moderate effect even at higher energies. Overall, the results demonstrate that incorporating rice husk ash improves gamma-ray absorption, particularly at low energies, while the MFP increases with energy due to the dominance of Compton scattering and reduced interaction cross sections [11].
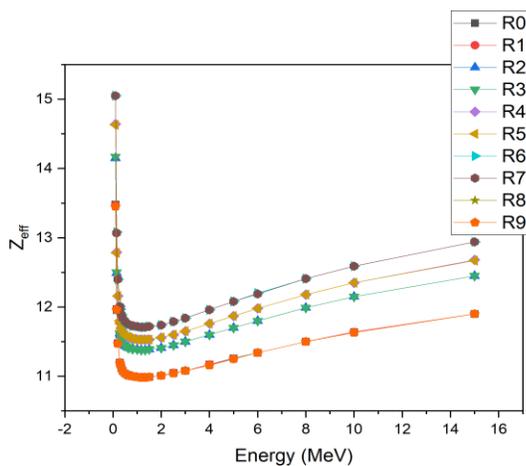

Fig.5: Comparison of the effective atomic number of rice husk ash-doped concrete at various energies.

Figure 5 presents the comparison of the effective atomic number of rice husk ash-doped concrete at various energies. The effective atomic number (Z_{eff}) of the rice husk ash–doped concrete, as shown in Table 4.7, exhibits a strong dependence on both photon energy and RHA content. At low photon energies (0.1–0.3 MeV), Z_{eff} increases with the RHA content, with samples R4–R7 showing the highest values (up to 15.05), reflecting the influence of heavier elements in the rice husk ash. This higher Z_{eff} enhances photoelectric absorption, improving gamma-ray shielding at low energies. As photon energy increases beyond 0.3 MeV, Z_{eff} gradually stabilizes for all samples, indicating that Compton scattering dominates photon interactions at intermediate energies and the effect of RHA composition becomes less pronounced. At higher energies (5–15 MeV), samples with greater RHA content maintain slightly higher

Z_{eff} values, suggesting a modest contribution of heavier elements to photon absorption even in the pair production energy range. Overall, these results confirm that incorporating rice husk ash effectively increases the effective atomic number of concrete, enhancing its gamma-ray shielding efficiency, particularly at low to medium photon energies.

4 Conclusion

The study demonstrates that rice husk ash–doped concrete is a viable and eco-friendly alternative for gamma radiation shielding. Incorporating RHA into concrete significantly enhances photon attenuation, particularly at low to medium energies (0.1–3 MeV), due to increased effective atomic number and density, which promote photoelectric absorption. Radiation shielding parameters, including mass attenuation coefficient, linear attenuation coefficient, half-value layer, tenth-value layer, and mean free path, indicate improved performance with higher RHA content. At higher photon energies (>5 MeV), Compton scattering and pair production dominate, causing differences among samples to diminish, although RHA-doped concretes maintain slightly higher shielding efficiency. Overall, the findings confirm that RHA not only serves as a sustainable cement replacement but also contributes to enhanced gamma-ray shielding, making it a promising material for sustainable and effective radiation protection applications.

References

[1] Akkurt, I., Akyıldırım, H., Mavi, B., Kilincarslan, S., & Basyigit, C. (2010). Photon attenuation coefficients of concrete, including barite, for different energy ranges. *Journal of Hazardous Materials, 176*(1–3), 642–647. https://doi.org/10.1016/j.jhazmat.2009.11.040

[2] Issa, S. A. M., Tekin, H. O., Erguzel, T. T., & Susoy, G. (2018). The investigation of gamma radiation shielding parameters of concretes containing different aggregates. *Radiation Physics and Chemistry, 144*, 120–126. https://doi.org/10.1016/j.radphyschem.2017.10.019

[3] Kharita, M. H., Takeyeddin, M., Alnassar, M., & Yousef, S. (2008). Development of special radiation shielding concretes using natural local materials and evaluation of their shielding characteristics. *Progress in Nuclear Energy, 50*(1), 33–36. https://doi.org/10.1016/j.pnucene.2007.10.004

[4] El-Taher, Atef., Zakaly, Hesham MH., Pyshkina, Mariia., Allam, EA., El-Sharkawy, R M Mahmoud, ME., Abdel-Rahman, Mohamed AE., (2021) A comparative Study Between Fluka and Microshield Modelling Calculations to study the Radiation-Shielding of Nanoparticles and Plastic Waste composites. Zeitschrift für anorganische und allgemeine Chemie 647 (10), 1083-1090.

[5] Allam, EA., El-Sharkawy, RM., El-Taher, Atef., Shaaban, ER., Massoud, EE., Mahmoud, ME., (2022) Enhancement and optimization of gamma radiation shielding by doped nano HgO into nanoscale bentonite. Nuclear Engineering and Technology 54, 6, PP. 2253-2261.

[6] El-Sharkawy, RM., Allam, EA., El-Taher, Atef., Elsaman, Reda., Massoud, EE., Mahmoud, ME., (2022) Synergistic effects on gamma-ray shielding by novel light-weight nanocomposite materials of bentonite containing nano Bi2O3 additive. Ceramics International 48 (5), 7291-7303.

[7] El-Sharkawy, RM., Allam, EA., El-Taher, Atef., Shaaban, E.R. and Mahmoud, ME., (2021) Synergistic Effect of Nano-bentonite and Nano cadmium Oxide Doping Concentrations on Assembly, Characterization and Enhanced Gamma-Rays Shielding Properties of Polypropylene Ternary Nanocomposites. International Journal of Energy Research. 45 (6), 8942-8959.

[8] Obam, S. O., & Egbe, N. O. (2011). Gamma-ray attenuation coefficients of some rocks and soils. *Journal of Environmental Radioactivity, 102*(9), 849–852. https://doi.org/10.1016/j.jenvrad.2011.05.004

[9] Sayyed, M. I., Issa, S. A. M., Tekin, H. O., & Saddeek, Y. B. (2017). Comparative study of gamma-ray shielding properties of different glass systems. *Materials Chemistry and Physics, 190*, 217–226. https://doi.org/10.1016/j.matchemphys.2017.01.025

[10] Tekin, H. O., Issa, S. A. M., Mahmoud, K. A., Erguzel, T. T., & Susoy, G. (2020). Phy-X/PSD: Development of a user-friendly online software for calculation of radiation shielding parameters. *Radiation Physics and Chemistry, 173*, 108861. https://doi.org/10.1016/j.radphyschem.2020.108861

[11] Taylor, H. F. W. (1997). Cement chemistry (2nd ed.). Thomas Telford Publishing.

[12] Berger, M. J., Hubbell, J. H., Seltzer, S. M., Chang, J., Coursey, J. S., Sukumar, R., Zucker, D. S., & Olsen, K. (2010). *XCOM: Photon cross sections database (NIST Standard Reference Database 8).* National Institute of Standards and Technology.

[13] El-Taher, Atef., Ali, AM., Saddeek, YB., Elsaman, R., Algarni, H., Shaaban, KS., Amer, T.Z., (2019) Gamma ray shielding and structural properties of iron alkali alumino-phosphate glasses modified by PbO. Radiation Physics and Chemistry, 165, 108403.

[14] Mahmoud, ME., El-Sharkawy, RM., Allam, EA., Elsaman, R., El-Taher, Atef., (2019) Fabrication and characterization of phosphotungstic acid-Copper oxide nanoparticles-Plastic waste nanocomposites for enhanced radiation-shielding. Journal of Alloys and Compounds 803, 768-777.

[15] Saddeek, Y.B., Shaaban, KH.S., Elsaman, Reda., El-Taher, Atef., Amer, T.Z., (2018) Attenuation-density anomalous relationship of lead alkali borosilicate Glasses. Radiation Physics and Chemistry 150, 182–188.

[16] Chandrasekhar, S., Satyanarayana, K. G., Pramada, P. N., Raghavan, P., & Gupta, T. N. (2003). Review processing, properties, and applications of reactive silica from rice husk—An overview. *Journal of Materials Science, 38*(15), 3159–3168. https://doi.org/10.1023/A:1025157114800

[17] El-Khayatt, A. M., & Akkurt, I. (2013). Photon interaction, effective atomic number, and electron density of some concrete materials. *Annals of Nuclear Energy, 62*, 132–137. https://doi.org/10.1016/j.anucene.2013.06.008

[18] Hubbell, J. H., & Seltzer, S. M. (2004). Tables of X-ray mass attenuation coefficients and mass energy-absorption coefficients. *NIST Standard Reference Database 126*.

[19] Kurama, H., & Topçu, I. B. (2004). Properties of the autoclaved aerated concrete produced from coal bottom ash. *Journal of Materials Processing Technology, 209*(2), 767–773. https://doi.org/10.1016/j.jmatprotec.2008.02.044

[20] U Rilwan, SA Edeh, MM Idris, II Fatima, SF Olukotun, GZ Arinseh, PZ Bonat, A. El-Taher, KA Mahmoud, Taha A Hanafy, MI Sayyed., (2025) Influence of waste glass on the gamma-ray shielding performance of concrete. Annals of Nuclear Energy 210, 110876.

[21] HH Negm, EA Allam, IM Nabil, E Abdeltwab, M Mostafa, A. El-Taher., (2024) Exploring the potential of attapulgite clay composites containing intercalated nano-cadmium oxide and nano-nickel oxide for efficient radiation shielding applications. Radiation Physics and Chemistry 225, 112149.

[22] Meshari Almeshari, Fawzy Hammad Sallam, Mohamed Tharwat, Yasser Alzamil, Mohammed Salih, Bader Alshoumr, Amjad Alyahyawi, Atef El-Taher., (2024) Preparation and structure investigation of polyethylene terephthalate polyester reinforced Ni0. 5Zn0. 5Fe2O4 nanoparticles for gamma ray shielding performance. Physica Scripta 99 (5), 055311.

[23] Hani H Negm, Rehab M El-Sharkawy, Eslam Abdeltwab, Massaud Mostafa, Mohamed E Mahmoud, Atef El-Taher., (2024) Evaluation of shielding properties of a developed nanocomposite from intercalated attapulgite clay by Cd/Pb oxides nanoparticles. Physica Scripta 99 (5), 055956.

[24] Ahmed Khalil, Ibrahim I Bondouk, Elhassan A Allam, Islam M Nabil, Mogahed Al-Abyad, Heba Saudi, Atef El-Taher, Mohamed E Mahmoud, Ahmed Amar., (2024) A binary composite material of nano polyaniline intercalated with nano-Fe2O3 for enhancing gamma-radiation-shielding properties: experimental and simulation study. Progress in Nuclear Energy 169, 105067.

[25] Feras Alafer, FH Sallam, Meshari Al Meshari, Yasser Alzamil, Ahmad Abanomy, Sultan Alhujaili, Atef El-Taher., (2024) The influence of thermal treatment on the structural properties and gamma rays shielding of

bentonite clay ceramic. Radiation Physics and Chemistry 217, 111531.

[26] U Rilwan, GM Aliyu, SF Olukotun, MM Idris, AA Mundi, S Bello, I Umar, A. El-Taher, KA Mahmoud., (2024) Recycling and characterization of bone incorporated with concrete for gamma-radiation shielding applications. Nuclear Engineering and Technology. 56, 7, 2828-2834.